13

Analysis of the failure mechanisms in magnesium–manganese dioxide dry cells

S. R. Narayanan*

Department of Chemistry, University of Exeter, Stocker Road, Exeter EX4 4QD (U K)

Abstract

Failure of high-energy magnesium–manganese dioxide dry cells is characterised by loss of ampere hour capacity on storage, increase of voltage delay, and anode corrosion The present investigation of the degradation of cell performance suggests several underlying mechanisms The important ones have been identified as redistribution of electrolyte in the cathode, breakdown of the passive film on the anode, and corrosion at bi-metallic interfaces formed by cell components These degradation processes tend to increase cell internal resistance, thereby reducing capacity output and increasing voltage delay An analysis of the dependence of ampere hour capacity and voltage delay on internal resistance of the cell has also been presented

1. Introduction

The magnesium–manganese dioxide ($Mg-MnO_2$) dry cell belongs to that class of primary cells with high energy density and long shelf life [1–4] This cell has found increasing application in man-pack communication sets employed in tropical parts, such as India and Indonesia. Due to its high power density, excellent capacity retention characteristics following extended periods of storage at elevated temperatures, and good, low-temperature performance, the $Mg-MnO_2$ dry cell is superior to the conventional $Zn-MnO_2$ (Leclanché type) cell. Further, the $Mg-MnO_2$ cell uses materials and technology which are relatively inexpensive compared with other commercially available high-energy systems based on lithium and zinc (alkaline type)

During the course of design, development, and optimisation of $Mg-MnO_2$ dry cells at Bharat Electronics, India, several modes of cell failure were investigated. The present study identifies and analyzes some of the important and common causes of failure Understanding of the physicochemical processes governing the failure mechanisms provides a scientific basis for performance optimisation and development of methods for early detection of failure

Cell construction

The $Mg-MnO_2$ dry cell studied in this work is of 'bobbin' type construction, shown in Fig. 1. This basic design is widely employed by the major ma-

---

*Present address MS 277-212, Jet Propulsion Lab , Caltech, 4800 Oak Grove Drive, Pasadena, CA 91109, U S.A
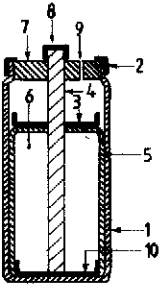
Fig 1 Construction of bobbin-type, cylindrical Mg–MnO$_2$ dry cell 1, Magnesium can, 2, steel collar, 3, top washer, 4, carbon-rod current collector, 5, kraft paper separator, 6, cathode bobbin of MnO$_2$, acetylene black, BaCrO$_4$, and electrolyte, 7, plastic seal, 8, tin-plated brass cap, 9, vent, 10, bottom washer

nufacturers such as Ray-O-Vac Inc , U S.A , Marathon Batteries Inc , U S A , and Bharat Electronics Ltd , India As the construction of the cell has a significant bearing on the failure mechanisms, a brief description of the construction is appropriate

The cylindrical magnesium can, extruded from AZ21 alloy, is the negative electrode and the cell container The inner surface of the can is passivated by a coating of corrosion inhibitors of proprietary composition (usually chromates and esters of fatty acids [2, 5, 8]) This passivation coating protects magnesium from electrolyte corrosion before discharge is initiated, and thereby endows the cell with long shelf life Breakdown of this insulating, protective passive film at the initiation of discharge, however, entails a delayed attainment of the operating voltage, a phenomenon referred to as delayed action or voltage delay [1–3] The role of the passive film and its electrochemical properties have been discussed extensively elsewhere [4–8] The cathode consists of manganese dioxide (85%), acetylene black (12%), barium chromate (2%), magnesium hydroxide (1%) blended with magnesium perchlorate solution (4 N) to a pasty consistency [1, 2] This cathode mix is consolidated to form a cylindrical bobbin (see Fig 1) The carbon rod serves as a current collector. A layer of kraft paper acts as a separator while the compression washer prevents the unfolding of the kraft paper that envelopes the cathode A brass cap pressed on to the carbon rod serves as an electrical contact. A plastic top seals the cell and is swaged firmly to the can by a tin-plated steel collar

3. Characteristics of performance and failure

A typical CD-size Mg–MnO$_2$ dry cell (height 90 mm, dia 22 mm) manufactured at Bharat Electronics Ltd , India, exhibits an open-circuit voltage of 2.0 V and delivers 2.5 A h at 25 °C, when discharged to 1 25 V at a constant current of 500 mA. The *voltage delay or delay time* (which is the time taken to attain a particular voltage following initiation of discharge)

up to 1 25 V is, typically, 0 3–0.5 s The internal resistance measured by a c and d c methods is in the range 0 3–1 0 Ω [5–7] Failure of such cells is characterised by:

    (a) anode corrosion during storage,

    (b) inability to deliver the specified capacity,

    (c) increase of delay time

The large negative reduction potential of magnesium ($E^\circ = -2\ 37$ V) makes it extremely susceptible to corrosion in the battery electrolyte. Corrosion of unpassivated magnesium alloys proceeds in a localised manner, resulting in pits and perforations that lead to leakage of electrolyte even before the cell has been discharged Corrosion of magnesium is aggravated by graphitic inclusions that result from the use of graphite as a lubricant during extrusion of the can Further, it has been found that the presence of impurities such as Fe^{2+}, Cd^{2+}, Cl^- and $ClO_3{}^-$ accelerate corrosion Thus a protective passivation coating is essential to the successful performance of the cell Unlike passive films on lithium in non-aqueous lithium batteries [9–11], the passivation coating cannot re-form following the termination of discharge Thus, once discharge is initiated, the cell has to be continuously discharged to recover the entire capacity

Corrosion of magnesium occurs according to the chemical reaction

$$Mg + 2H_2O \longrightarrow Mg(OH)_2 + H_2$$
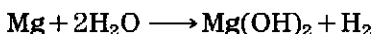
Consequently, corrosion reduces the water content of the electrolyte and produces insoluble and non-conducting $Mg(OH)_2$ Therefore, as corrosion proceeds, the internal resistance of the cell increases The results of an experimental study on intermittent discharge characteristics (shown in Table 1) demonstrate that with increasing duration of discharge, the recovered capacity decreases Experimental results presented below also suggest that several other failure modes lead to an increase of the cell's internal resistance, resulting in reduced capacity output It is therefore of use to analyse the dependence of ampere hour capacity on internal resistance of the Mg–MnO$_2$ dry cell.

TABLE 1

Intermittent discharge characteristics of 15 V, 7 0 A h Mg–MnO$_2$ dry battery (Bharat Electronics, India) discharged at 250 mA, 25 °C Results averaged over three batteries in each case

Duration of discharge (hours/day)	Capacity under continuous discharge (%)
6 0	99
4 0	98
2 0	95
1 0	72
0 5	53

## 4. Dependence of ampere hour capacity on the internal resistance of the cell

Consider an Mg–MnO$_2$ dry cell being discharged at a constant current, I The closed circuit cell voltage, V, is related to the open circuit cell voltage V_o by

$$V = V_o - IR_{int} \qquad (1)$$

where R_{int} is the equivalent internal resistance for the cell The internal resistance of the cell is a lumped parameter consisting of the polarisation resistances at the anode and cathode, resistance of the passive film, resistance of the electrolyte, current collectors, and electrical contacts [5] The open-circuit voltage of the cell, V_o, may be expressed as,

$$V_o = E_c - E_a \qquad (2)$$

where E_c and E_a are the equilibrium potentials of the positive (cathode) and negative (anode) electrodes, respectively. The MnO$_2$ electrode sustains the discharge reaction [1]
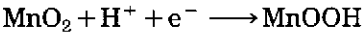
$$MnO_2 + H^+ + e^- \longrightarrow MnOOH$$

and therefore the equilibrium potential may be expressed by the Nernst equation

$$E_c = E_c^{\,o} + \frac{RT}{F} \ln \frac{a_{MnO_2} a_{H^+}}{a_{MnOOH}} \qquad (3)$$

where a_{MnO_2}, a_{H^+}, a_{MnOOH} refer to the activities of the respective substances. Since the pH of the MnO$_2$ electrode is constant (buffered to about 8 0 by Mg(OH)$_2$), eqn (3) may be rewritten as,

$$E_c = E_c^{\,o'} + \frac{RT}{F} \ln \frac{a_{MnO_2}}{a_{MnOOH}} \qquad (4)$$

where

$$E_c^{\,o} = E_c^{\,o} - \frac{RT}{F} \, pH$$

The equilibrium potential of the magnesium electrode is a mixed potential and may be represented by E_{cor}, the corrosion potential of magnesium in the electrolyte
In the practical situation the cathode limits the capacity of the Mg–MnO$_2$ cell Let Q_o be the theoretical capacity of the cathode and Q the capacity actually withdrawn from the cell Then, from eqns (2) and (4),

$$V_o = E_c^{\,o'} - E_{cor} + \psi \, \frac{RT}{F} \ln \frac{Q_o - Q}{Q} \qquad (5)$$

where the factor ψ takes into account the non-ideality of the mixture of MnO$_2$ and MnOOH [13, 14]. ψ has typical values in the range 1–2
Thus, when the cell is at 50% state-of-charge, $a_{MnO_2} = a_{MnOOH}$, $Q = Q_o/2$ and $V_o = E_c^{\,o'} - E_{cor}$ Therefore eqn (1) becomes·

$$V = E_c^{\circ'} - E_{cor} + \left(\psi \frac{RT}{F} \ln \frac{Q_o - Q}{Q} \right) - IR_{int} \tag{6}$$

Let Q_{cf} be the capacity withdrawn up to a voltage of V_{cf} (usually termed the cut-off voltage). Under these conditions,

$$V_{cf} = E^{\circ'} - E_{cor} + \left(\psi \frac{RT}{F} \ln \frac{Q_o - Q_{cf}}{Q_{cf}} \right) - IR_{int} \tag{7}$$

Re-arranging eqn. (7) and substituting $E_c^{\circ'} - E_{cor} = V'$,

$$\frac{Q_{cf}}{Q_o} = \frac{1}{1 + \exp\left\{ (V_{cf} - V' + IR_{int}) - \dfrac{F}{\psi RT} \right\}} \tag{8}$$

Equation (8) relates the capacity recovered at a particular *cut-off* voltage to the internal resistance and the theoretical capacity of the cell. The theoretical dependence of Q_{cf}/Q_o on IR_{int} for various values of V_{cf} according to eqn (8) is shown graphically in Fig. 2 for $V' = 1.6$ V This value of V' has been arrived at from experimental measurements of V_o at 50% state-of-charge, and E_{cor} For example, it is seen from Fig 2 that significant loss of capacity may be expected for $V_{cf} = 1$ 2 V when IR_{int} exceeds 0.35 V. Therefore, for a typical discharge current of 250 mA, R_{int} should not exceed 1.4 Ω. Equation (8) can therefore be used to estimate the limiting values of internal resistance
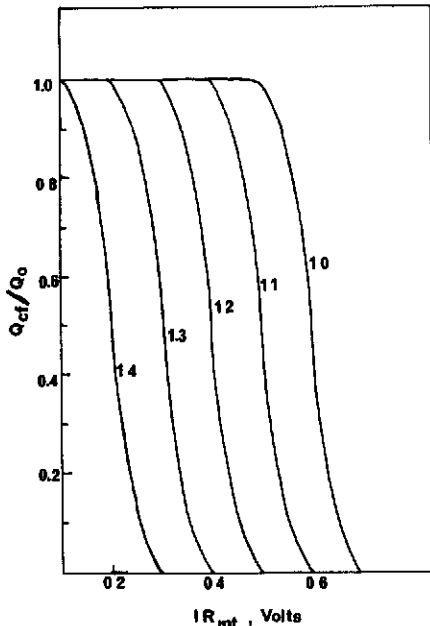

Fig 2 Theoretical dependence of Q_{cf}/Q_o on drop across internal resistance, IR_{int}, at different values of cut-off voltage, V_{cf}, shown on the curves, $\psi = 1$

permissible if a definite capacity is to be recovered at a chosen discharge current. Consequently, any mechanism that operates to increase the internal resistance would reduce the capacity recovered from the cell in a manner governed by eqn (8)

Voltage delay in the Mg–MnO$_2$ dry cell (the time taken to attain a particular steady operating voltage following initiation of discharge) is governed by the rate at which the protective anode film breaks down [2, 3, 12] During discharge across a constant resistance R_L, the discharge current and cell voltage are governed by the following relations

$$I = \frac{V_o}{R_{int} + R_L} \tag{9}$$

$$V = V_o \left(\frac{R_L}{R_{int} + R_L} \right) \tag{10}$$

During the initial moments of discharge, the internal resistance is almost entirely governed by the resistance of the passive film [12] Thus, increase of the passive film resistance would result in a lowered initial discharge current It has been shown [12] that a reduced initial discharge current leads to an enhanced voltage delay. Any mechanism therefore that increases the resistance of the anode film would increase the delay time. Subsequent to anode film breakdown, the internal resistance would be governed by mass-transfer polarisation at the cathode and the anode/electrolyte interfaces, resistance of the electrolyte, current collectors, and electrode contacts Therefore, an increase in these contributions to the internal resistance would result in reduced cell voltages (eqn (10)) and more delay before a particular cell voltage is reached

5. Mechanisms underlying increase of internal resistance

5 1 Redistribution of electrolyte

In the course of studies on design optimisation it was observed that Mg–MnO$_2$ cells suffered 30–40% loss of capacity and a ten-fold increase in voltage delay during the first four weeks after manufacture When cut open, the cells confirmed the absence of an electronic short or of corrosion of the anode However, when about 0.5 ml of distilled water was injected into each of the cells through the vent, and the cells discharged after 24 h, 95% of the *first-day* capacity was recovered The voltage delay simultaneously fell to about 0 5 s Cells injected with 0 5 ml of distilled water also showed a stabilised capacity in the subsequent weeks of storage

These observations may be understood in terms of reorganisation of electrolyte in the cell during the period of storage The wetting of the pores of acetylene black and manganese dioxide particles, being a rate process, could remain incomplete at the end of the blending of the cathode mix (an operation which typically takes 30 min) Slow redistribution of the electrolyte

into the pores during the weeks following manufacture would result in loss of ionic contact between particles, leading to an increase in the internal resistance of the cell, consequent loss of capacity, and also an increase in voltage delay. This situation is depicted in Fig. 3 When electrolyte containing 0.5% of a non-ionic surfactant was used, capacity loss on 3 months storage was less than 5% with no detectable change in voltage delay It may thus be concluded that the surfactant appears to promote wetting of the pores, thus allowing for more complete absorption of the electrolyte and reducing the scope for subsequent reorganisation Also, for the same amount of electrolyte used, the cathode blend containing the surfactant appeared drier, suggesting reduction in the amount of *free* electrolyte. The effect of injecting small quantities of water during the week following manufacture, and the result of adding small amounts of surfactant to the electrolyte are, therefore, both consistent with the mechanism of electrolyte reorganisation as the basic cause of failure

5 2. Cell dry-out during extended periods of storage

It has been observed that $Mg-MnO_2$ cells stored for over 3 years under ambient conditions exhibited loss of capacity to the extent of 90% and voltage delay as high as 3–10 min Non-destructive radiographic examination of the stored cells showed (Fig 4(a)) the presence of fissures in the cathode*. When cut open, the cells showed absence of anode corrosion, but presented a relatively dry cathode and separator. When each of these cells was injected with 2–3 ml of distilled water and discharged after 24 h, 80% of the specified capacity was recovered. Also, the cells exhibited a voltage delay of 0 5 s, which is the value specified for freshly manufactured cells. Radiographic examination of the cells injected with water suggested complete disappearance of the fissures (Fig. 4(b))

These observations suggest that cell dry-out leads to an increase in internal resistance, resulting in reduced capacity output and enhanced voltage
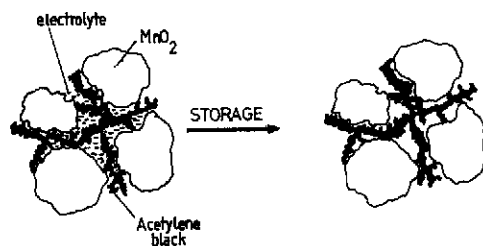

Fig 3 Schematic depiction of redistribution of electrolyte within pores of the cathode mix The particles of acetylene black are depicted as porous and about ten times smaller than the particles of MnO_2

---

*Since magnesium has a low cross-section for X-ray absorption compared with the other components of the cell, investigation of the inner details of the cell is possible The situation may be quite different for the $Zn-MnO_2$ cells
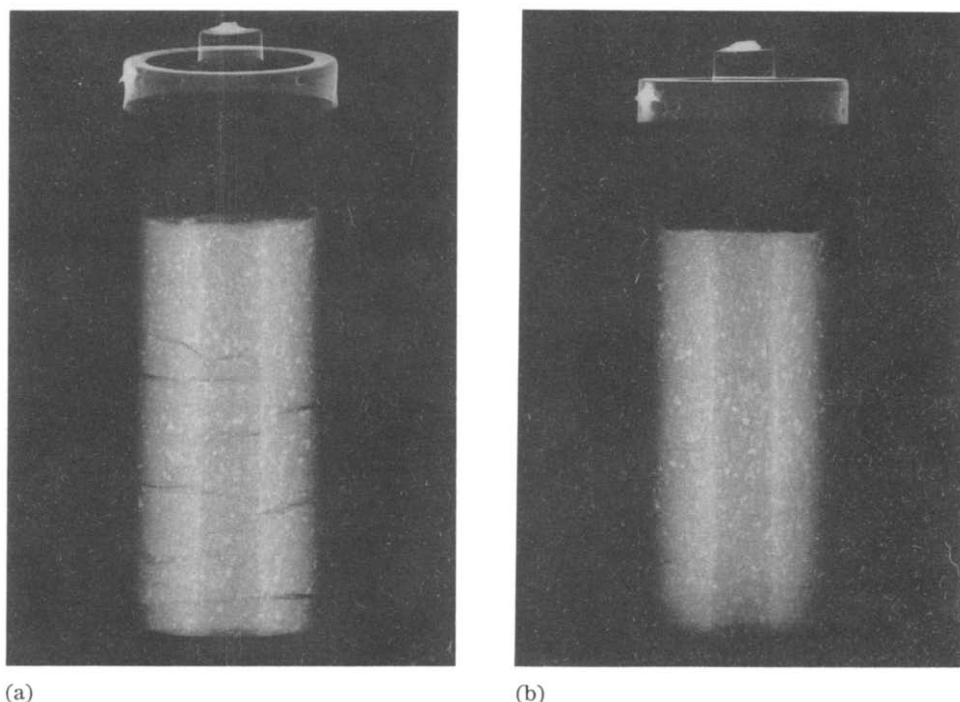
(a)   (b)

Fig 4 X-radiographic image of Mg–MnO$_2$ dry cell stored for 3 years under ambient conditions
Radiographic imaging conditions 95 kV, 1 mA, 0 6 m between object and source, NDT-70
Indu film with exposure of 1 min The bright spots are strongly absorbing particles of barium
chromate (b) X-radiograph of cell in (a), 24 h following injection of 2 ml of distilled water

delay The cell, not being hermetically sealed, provides several pathways for
loss of water by evaporation Improvements in mechanical aspects of cell
design are necessary to avert failure by this mode Also, by improvements
in anode-efficiency, the production and accumulation of hydrogen within the
cell may be reduced and the vent may possibly be eliminated

5 3 Corrosion at the brass cap

Loss of capacity to the extent of 80% was observed in battery packs
containing cells where corrosion was observed at the junction of the brass
cap and the carbon rod This may be understood as follows

The partially graphitised carbon rod current collector (Fig 1) is usually
impregnated with about 5% w/w of paraffin wax to prevent creepage of
electrolyte by capillary action However, when the compression of the cathode
bobbin exceeds a threshold limit (equivalent to a density of approximately
1.80 g cm^{-3}) electrolyte is forced up to the top of the carbon rod and
reaches the brass cap (see Fig 1) The corrosion that follows is explained
by the values of mixed potentials* for the cell components in the electrolyte,

---

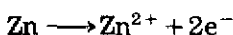*Also referred to as galvanic potentials in the terminology used in corrosion research

TABLE 2

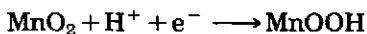Mixed potentials of components of the Mg–MnO$_2$ dry cell in 4 N Mg (ClO$_4$)$_2$ vs calomel electrode (0 1 N MgCl$_2$) at 25 °C

Component	Mixed potential (V)
Tin-plated brass cap	−0 363
Steel collar	−0 400
Passivated Mg can	−1 524
MnO$_2$ cathode	+0 565

shown in Table 2. The difference in the mixed potentials for the brass cap and the carbon rod carrying the MnO$_2$ cathode is $+0.565 - (-0.363)$, i.e., 0.928 V This being significantly positive, corrosion of the brass cap may be expected. The conjugate reactions of corrosion would be:

anodic reactions:

$$Cu \longrightarrow Cu^{2+} + 2e^-$$

$$Zn \longrightarrow Zn^{2+} + 2e^-$$

$$Sn \longrightarrow Sn^{4+} + 4e^-$$

cathodic reactions.

$$MnO_2 + H^+ + e^- \longrightarrow MnOOH$$

$$O_2 + 4H^+ + 4e^- \longrightarrow 2H_2O$$

The low polarisability of the MnO$_2$ electrode and the unfavourable area ratio of corroding metal to cathodic reaction sites are ideal situations for very rapid corrosion. However, the significantly lower rates of corrosion observed are due to the ohmic control arising from the restricted capillary rise of electrolyte.

Following the initiation of corrosion, insulating corrosion products (carbonates and hydroxides of Cu, Zn, Sn) accumulate at the junction, and the internal resistance* of the cell typically rises from about 0.5–20 Ω. In some cases there is total loss of electrical contact This form of brass cap corrosion is insidious as it occurs totally unseen from below and is of immense consequence, as the entire current during cell discharge passes across the junction of the brass cap and the carbon rod
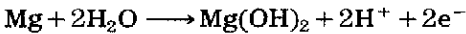
Control of compaction of the cathode bobbin and reduced electrolyte levels minimise this mode of failure Application of conductive hydrophobic barrier coatings (based on carbon black dispersed in synthetic rubber solutions) prevents access of the electrolyte to the carbon rod without contributing significantly to the internal resistance of the cell. The use of higher levels of wax content tends to increase the resistance of the carbon rod.

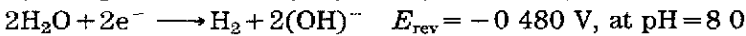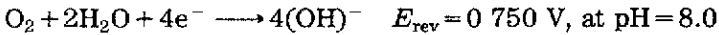*Internal resistance measured by the steady-state d c method described in ref 6

5 4 Corrosion of the steel collar

Under conditions of relative humidity greater than 80%, as, for example, in the simulation of jungle storage* conditions, corrosion has been observed at the junction of the steel collar and the can This is initiated by the creepage of the electrolyte to the junction From Table 2, the difference between the mixed potentials for the magnesium can and the steel collar is $-0\ 400-(-1\ 524)$, i e , $1\ 124$ V At these positive potentials, corrosion of magnesium can be expected and the conjugate reactions of corrosion are

Anodic reaction·

$$Mg + 2H_2O \longrightarrow Mg(OH)_2 + 2H^+ + 2e^-$$

Cathodic reactions:

$$O_2 + 2H_2O + 4e^- \longrightarrow 4(OH)^- \quad E_{rev} = 0\ 750 \text{ V, at pH} = 8.0$$
$$2H_2O + 2e^- \longrightarrow H_2 + 2(OH)^- \quad E_{rev} = -0\ 480 \text{ V, at pH} = 8\ 0$$

Once corrosion is initiated, propagation is restricted only by the availability of electrolyte Accumulation of corrosion products aggravates corrosion by wicking up the electrolyte to the junction Corrosion is often found to be initiated at a location remote from the junction itself, as, for example, on the body of the can facing the cathode. This is because the initiation of corrosion occurs by breakdown of the anode film, and this happens where the film is weakest The accumulation of corrosion products at the above mentioned junction results in significant loss of capacity and increase of voltage delay, as the entire discharge current traverses the junction of the steel collar and the can Even a barely visible film of corrosion products has been found to increase the internal resistance to as high as $10\ 0$ Ω, reducing performance drastically

5 5 Internal electronic short

An internal electronic short in Mg–MnO$_2$ dry cells is usually a consequence of assembly defects which result in the anode and cathode coming into direct electronic contact. These defects are, commonly, (a) separator or bottom washer incompletely enclosing the cathode, (b) particles of the cathode mix appearing above the top washer (see Fig 1) and bridging the anode to cathode gap Under these conditions, cell discharges at a rate governed by the equivalent resistance of the electronic short, R_e, and the self-discharge current I_e would be given by

$$I_e = \frac{V_o}{R_{int} + R_e} \tag{11}$$

Such a direct dissipation of capacity is well recognised as a failure mode for all types of cells However, when an Mg–MnO$_2$ dry cell with an internal electronic short is part of a battery pack, the consequences are more far-

---

*As per U S Military Specifications

reaching. For example, in the battery pack of Fig. 5, the cells of branch B discharge across R_e and cells 1, 3, 4 of branch A tend to get charged. Apart from the capacity dissipation which results, it is known that [4] discharge currents greater than 10^{-8} A cm^{-2} (anode area) are sufficient to break down the passive film on the anode Thus the anode film in cells 5–8 (Fig. 5) is induced to break down and unrestricted corrosion of the cells could be expected, leading to extensive loss of capacity and increase of voltage delay.

In an experimental study, 20 battery packs (consisting of 16 CD-size Mg–MnO$_2$ cells in two parallel rows of eight) were stored for 3 months under ambient conditions and then discharged. Ten of these packs had been wired with one cell (occupying a similar position in all the packs), carrying a 50 kΩ resistance across it, simulating a mild electronic short. For the packs with a simulated electronic short the capacity recovered for a discharge load of 100 Ω was 40–60% of that of the normal packs, and the voltage delay when discharged across 10 Ω and measured up to 10 8 V was 10–20 times that of the normal packs Thus cells with an internal electronic short cause all the other cells of the battery pack to fail.

6. Conclusions

The failure of Mg–MnO$_2$ dry cells is most commonly caused by an increase in cell internal resistance. The important mechanisms underlying this failure mode have been identified with reorganisation of electrolyte and cell dry-out, as well as electrochemical corrosion processes at bi-metallic junctions. Theoretical analysis of the dependence of ampere hour capacity on the internal resistance provides a basis for assessing the effect of increase in internal resistance Experimental results suggest that electrolyte reorganisation may be prevented by the addition of surfactants to the electrolyte Corrosion of the brass cap/carbon rod and steel collar/magnesium can interfaces can be precluded if electrolyte creepage to these interfaces is prevented. The presence of a mild electronic short in just one cell is detrimental to the performance of the entire battery pack (having cells wired in series and parallel)

These results demonstrate and emphasise how some of the basic aspects of cell design are crucial to cell performance. The approach followed here
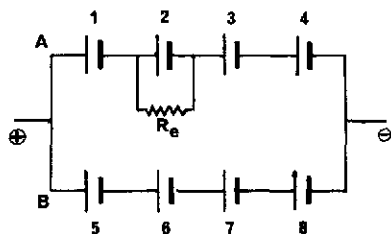

Fig 5 Schematic of battery pack carrying an Mg–MnO$_2$ dry cell with an internal electronic short represented by a resistance across the cell

may be extended to other battery systems with similar electrochemical and constructional features.

Acknowledgements

References

1 J. L. Robinson, in N. C. Cahoon and G. W. Heise (eds.), *The Primary Battery*, Vol. II, Wiley-Interscience, New York, 1976.
2 B. V. Ratnakumar and S. Sathyanarayana, *J. Power Sources, 10* (1983) 219.
3 S. Sathyanarayana and B. V. Ratnakumar, *J. Power Sources, 10* (1983) 243.
4 S. R. Narayanan and S. Sathyanarayana, *J. Power Sources, 15* (1985) 27.
5 S. R. Narayanan and S. Sathyanarayana, *J. Power Sources, 24* (1988) 51.
6 S. R. Narayanan and S. Sathyanarayana, *J. Power Sources, 24* (1988) 295.
7 S. R. Narayanan and S. Sathyanarayana, *J. Electroanal. Chem., 265* (1989) 103.
8 B. V. Ratnakumar, *J. Appl. Electrochem., 18* (1988) 268.
9 A. N. Dey, *Thin Solid Films, 43* (1977) 31.
10 C. R. Schlaijker, in J. P. Gabano (ed.), *Lithium Batteries*, Academic Press, London, 1983.
11 E. Peled, *J. Power Sources, 9* (1983) 253.
12 S. R. Narayanan and S. Sathyanarayana, *J. Appl. Electrochem., 19* (1989) 495.
13 S. Sathyanarayana, *Trans. Soc. Adv. Electrochem. Sci. Technol., 11* (1976) 40.
14 W. C. Maskell, J. E. A. Shaw and F. L. Tye, *J. Power Sources, 8* (1982) 113.